

Direct observation and control of the Walker breakdown process during a field driven domain wall motion

S. Glathe,¹ R. Mattheis,^{1,a)} and D. V. Berkov²

¹IPHT Jena, A.-Einstein-Str. 9, 07745 Jena, Germany

²Innovent e.V., Prüssingstr. 27, 07745 Jena, Germany

(Received 12 June 2008; accepted 3 August 2008; published online 22 August 2008)

We report the real-time study of a domain wall motion in giant magnetoresistance nanostraps. We have visualized the Walker breakdown process (WBP) [N. L. Schryer and L. R. Walker, *J. Appl. Phys.* **45**, 5406 (1974)] in single shot experiments. The domain wall motion above the Walker breakdown is highly nonperiodic. Surprisingly, the time intervals of movement are equal or larger than those where the domain wall nearly stops. When an additional transversal magnetic field is applied, domain wall motion becomes more regular, enabling the study of the WBP in more detail. A sufficiently large transverse field can suppress the WBP completely. © 2008 American Institute of Physics. [DOI: 10.1063/1.2975181]

The domain wall (DW) motion was already examined theoretically using a one-dimensional (1D) model in the 1970s by Schryer and Walker.¹ They predicted an instability of the laminar movement of the DW above a critical value of the external field, the so-called Walker field H_w . An experimental evidence of a Walker breakdown process (WBP) in nanowires was found by Beach *et al.*² They verified the expected velocity-field relationship. More insight was gained by studying the transition time t_w the DW needs to move through the laser spot diameter used for the NANOMOKE analysis. Yang *et al.*³ observed large variations in t_w above WB, indicating velocity changes caused by the WB. Oscillation of the anisotropic magnetoresistance (AMR) amplitude during a DW motion observed by Parkin and co-workers^{4,5} indicates a periodic transition between a transverse wall and a vortex wall.

Our studies of the DW motion were performed in giant magnetoresistance (GMR) stacks used in modern applications, e.g., multiturn counters.⁶ This enabled us to characterize the DW motion in the single shot mode and therefore allowed the direct visualization of the WBP. Experiments were carried out by analyzing the temporal resistance evolution in giant magnetoresistive stacks of seed/12PtMn/2.5CoFe/0.8Ru/2.5CoFe/2Cu/0.5CoFe/20NiFe/5Ta prepared by direct current (dc) magnetron sputtering. A $d=20$ nm thick (“sense”) Permalloy (Py-NiFe) layer was used to study the DW movement. Nanowires of widths w between 160 nm and 1 μm and a length of $L=45$ μm were fabricated by photolithography and Ar ion etching under tilt. Electrical contacts provided by Au pads were manufactured by a lift-off process. The whole structure was protected by a 200 nm Al_2O_3 layer.

Magnetization reversals were induced by applying a linearly increasing magnetic field H_{long} [$dH_{\text{long}}/dt \sim 160$ (kA/m)/s] antiparallel to the magnetization direction of the sense layer. If the nucleation field is reached, a DW is nucleated on one end of the nanostrap and moves within several hundreds of nanoseconds through the complete nanostrap without pinning. Within this time interval the longitudinal field H_{long} is practically constant. Additionally, a constant transverse magnetic field H_{tr} , directed perpendicular

to the strip axis, is applied before H_{long} . The critical longitudinal field H_{long} (acting as the driving field of the DW motion) depends on the applied constant transversal field H_{tr} .⁷ The nucleation field H_{nuc} of the DW is then a sum of both fields ($H_{\text{nuc}}^2 = H_{\text{long}}^2 + H_{\text{tr}}^2$).

Our experimental setup is shown in Fig. 1. The system was fed by a dc over the dc path of a bias-T. By changing the magnetization state of the GMR sense layer, we obtained a voltage change over the GMR wire. The latter was measured over the radio frequency (rf) path of the bias-T by a rf amplifier and a digital oscilloscope (bandwidth of 6 GHz and sample rate of 40 Gsamples/s) in a single shot mode. Because the magnetization of the reference layer is parallel to the x -axis, a specific voltage value corresponds to a unique position of the DW in the nanostrap. Thus we can directly measure the DW motion along the strip. The signal to noise ratio was improved by a Hamming-based finite impulse response filter with a relative cut-off frequency $f_n/f_s=0.02$ (sample frequency was $f_s=40$ GHz) and a length of $N=400$ points.

We have also performed micromagnetic simulation of the DW motion with the commercially available MICROMAGNUS (Ref. 8) package in a Py nanowire with lateral sizes w

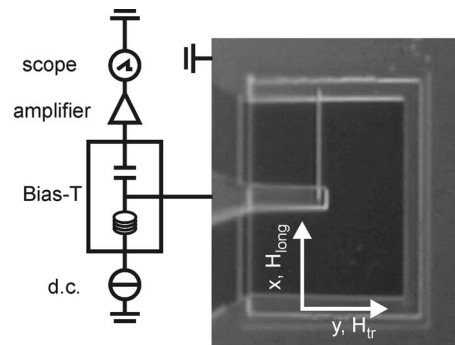


FIG. 1. Experimental setup used for the measurement of DW movement in the single shot mode. The directions of the two magnetic fields ($H_{\text{long}}, H_{\text{tr}}$) are marked. The system is fed by the dc over the dc path of the bias-T. By reversing the magnetization of the GMR stack sense layer, the resistance of the GMR stack changes. The accompanied voltage change in the system can be measured over the rf path of the bias-T using the rf amplifier and the oscilloscope.

^{a)}Electronic mail: roland.mattheis@ipht-jena.de.

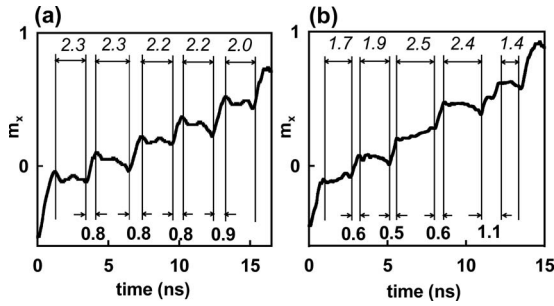


FIG. 2. Simulation of field driven DW dynamics in Py nanostrips ($w=200$ nm, $d=10$ nm, and $L=2000$ nm) for $H_{tr}=0$ kA/m: (a) with perfect borders ($H_{long}=4$ kA/m) and (b) with the edge roughness ($H_{long}=6.3$ kA/m).

$\times L=200 \times 2000$ nm² and a thickness of 10 nm (using cubic discretization cells with the side of 5 nm). The starting configuration contains a relaxed transversal DW at position $x=L/4$. To estimate the influence of edge roughness on the DW motion, we performed simulations of a wire with a stochastic edge roughness. For this purpose the magnetization of every cell within the edge zone of 20 nm width was disturbed using the Gaussian random process with the correlation length of 20 nm (comparable to the grain size of our films). With this roughness we obtained a wire coercivity $H_c=12$ kA/m, comparable to H_c found experimentally. Figure 2 shows the time evolution of the average x -component of the magnetization for wires (a) with perfect edges and (b) with an edge roughness. Whereas for the perfect wire a regular periodic behavior was found, the edge roughness leads to a more nonperiodic one. Such behavior inhibits the examination of WB by means of averaging many single experiments and allows only the single shot mode.

Figure 3 shows the voltage-time dependence caused by a DW motion in a 1 μ m wide nanostrip, which has a nucleation pad at one end to reduce the nucleation field and to allow the study of a DW motion at low driving fields, here 1.9 kA/m. The typical stepwise motion of a DW driven by fields larger than the WB field H_W is clearly visible. However, as predicted by simulations, the behavior of the DW during the WBP is highly irregular. This is confirmed by the signal spectrum [inset in Fig. 3(a)]. For a highly periodic process one would expect several sharp spectral peaks,

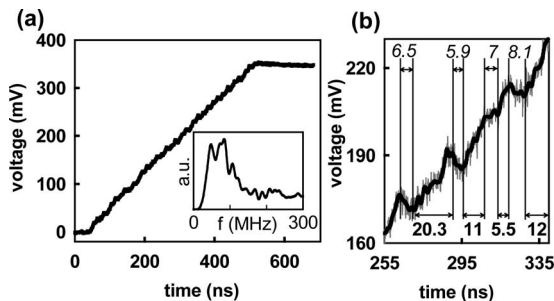


FIG. 3. (a) DW motion in the 1 μ m wide nanostrip with the nucleation pad ($H_{long}=1.9$ kA/m, $H_{tr}=0$ kA/m, and $v_{mean}=100$ m/s). Inset: frequency spectrum of the DW motion filtered with the Hamming filter ($N=50$ and $f_n/f_s=0.0025$). (b) Magnification of the DW movement for 85 ns corresponding to the distance of 8.5 μ m. Time periods of the fast forward motion and the slow or backward motion are marked. Gray line represents the original data and black line represents data obtained by using the Hamming filter.

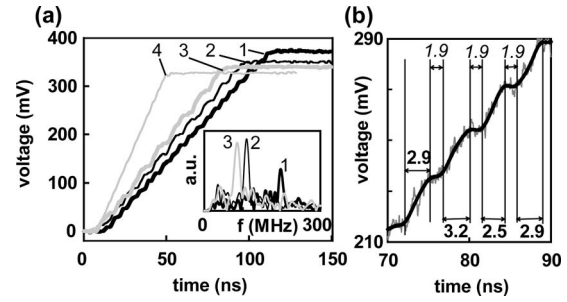


FIG. 4. (a) DW movement in the 250 nm wide nanostrips for several transverse fields: (1) $H_{tr}=12$ kA/m, $H_{long}=5.2$ kA/m, $v_{mean}=450$ m/s, and $v_{max}=760$ m/s; (2) $H_{tr}=16$ kA/m, $H_{long}=4$ kA/m, $v_{mean}=510$ m/s, and $v_{max}=930$ m/s; (3) $H_{tr}=18$ kA/m, $H_{long}=3.8$ kA/m, $v_{mean}=600$ m/s, and $v_{max}=980$ m/s; and (4) $H_{tr}=20$ kA/m, $H_{long}=3.3$ kA/m, and $v_{mean}=v_{max}=1060$ m/s. Inset: frequency spectrum of the DW motion filtered with the Hamming filter ($N=50$ and $f_n/f_s=0.0025$) for the cases specified above. (b) Details of the DW motion for (1) $H_{tr}=12$ kA/m. Gray line represents the original data and black line represents data obtained using the Hamming filter. Time of fast forward motion and halt is marked.

whereas we find a broad-band spectrum between 20 and 80 MHz.

Figure 3(b) shows a time period of 85 ns, corresponding to a traveling distance of about 8.5 μ m, visualizing a repeated backward and forward motion of the DW during the WBP. This indicates that a vortex (and not an antivortex) is nucleated and moves across the wire.⁹ In our experiments the periods of a rapid DW motion are roughly equal or even larger compared to periods when the wall nearly stops. This is in contrast to numerical simulations, where the motion periods are much shorter than the periods at halt. There are small voltage fluctuations (in the order of 5 mV) at time scales of 5 ns. These fluctuations correspond to changes in the DW position of around 500 nm, one-half of the nanostrip width. At present we believe that these variations are purely caused by noise and do not reflect real DW movement.

To study the WB in more detail we changed the anisotropy field H_K , which is one of the critical parameters determining the WB field:¹⁰ $H_W=\alpha H_K/2$ (α is the Gilbert damping factor). To change H_K we used nanostrips of different widths (160 nm, 250 nm, 500 nm, and 1 μ m). We also performed experiments with an additional transverse magnetic field H_{tr} . The application of this field has several effects. First, the longitudinal field H_{long} needed to induce the DW motion reduces with increasing H_{tr} . Second, the transverse field changes the WB field as shown by micromagnetic simulations.¹¹

Figure 4(a) shows single shot voltage-time dependencies of the DW motion in the 250 nm wide nanostrip above and below the WB for different transverse fields H_{tr} . It can be seen that we are able to control the WBP by means of the transverse field. For $H_{tr}=12$ kA/m the typical stepwise motion representing the WBP is visible. With increasing H_{tr} the number of WB events goes down. This can also be seen in the frequency spectrum [inset in Fig. 4(a)] as a reduction in frequencies of the WBP. At the highest applied transverse field ($H_{tr}=20$ kA/m) where the WBP is suppressed completely we do not find a peak in the spectrum. In contrast to the case without H_{tr} (see Fig. 3) the process is much more regular and a single frequency is clearly established. This could be caused by the effect of the DW broadening with

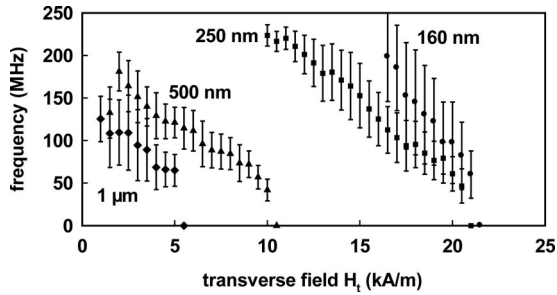


FIG. 5. Dependence of the WBP frequency on the transverse field for different nanostrip widths w .

increasing H_{tr} ,⁷ which leads to a smearing out of the edge roughness effect.

It is remarkable that here the maximum velocity increases with decreasing H_{long} . This is caused by the increased transverse field H_{tr} necessary for the reduction in H_{long} . An increased H_{tr} causes an enlargement in the DW width Δ . As predicted by the well established 1D model,^{1,10} the velocity of a DW is proportional to its width, which is under our experimental conditions responsible for the observed behavior. A detailed analysis of this effect is given in Ref. 7. Figure 4(b) shows details of the DW motion for a transverse field $H_{tr}=12$ kA/m. In contrast to the $1 \mu\text{m}$ wide nanostrip, we do not find the backward motion during the antivortex or vortex movement. However, the periods at motion are still longer than the periods at halt.

Figure 5 collects the frequencies of the WBP for different nanostrip widths. The error bars show the dispersion of the observed frequencies for the sets of different experiments performed under the same experimental conditions on the same sample. This indicates the stochastic behavior of the DW motion during WBP. One can state that the smaller the nanostrip is, the higher the transverse field needed to resolve and finally to suppress WB events. There are two reasons for this effect. First, the anisotropy H_K decreases with the decreasing ratio w/d , reducing the WB field $H_W = \alpha H_K / 2$. Second, the coercive field and thus the nucleation field (which is in our experiments the driving field of the DW) increase drastically with decreasing w . Summarizing, the difference $(H^2 - H_W^2)$ increases with decreasing w/d , and therefore frequencies of the WBP $\{f = \gamma_0 (H^2 - H_W^2)^{1/2} / [2\pi(1 + \alpha^2)]\}$ (Refs.

1 and 10) increase. Due to the nanostrip length ($45 \mu\text{m}$) resulting in the limited spatial resolution (determined by the resolution of the resistance measurements) we cannot detect WB events occurring at frequencies $f > 250$ MHz. Applying a transverse field, the difference $(H^2 - H_W^2)$ is reduced and the WBP can be detected with lower frequencies, whereas we need higher H_{tr} for smaller w/d .

Concluding, we have provided a direct evidence of the WBP by single shot measurements of a DW motion. This is necessary for nanostrips in GMR stacks where due to the interlayer magnetic interaction (orange peel coupling) and the edge roughness induced by the fabrication process, the WBP loses its periodic behavior. For $1 \mu\text{m}$ wide nanostrips we have found a backward motion of the DW, indicating a vortex formation during the WBP. By applying transverse fields we can control the WBP and even suppress it with sufficiently high transverse fields. With increasing H_{tr} the process becomes more periodic, which can be understood as the result of a DW broadening and the accompanying smearing out of the edge roughness effects.

We thank Novotechnik (Ostfildern, Germany) for financial support and J. Paul (Sensitec GmbH, Mainz, Germany) for sample preparation.

¹N. L. Schryer and L. R. Walker, *J. Appl. Phys.* **45**, 5406 (1974).

²G. S. D. Beach, C. Nistor, C. Knutson, M. Tsoi, and J. L. Erskine, *Nat. Mater.* **4**, 741 (2005).

³J. Yang, C. Nistor, G. S. D. Beach, and J. L. Erskine, *Phys. Rev. B* **77**, 014413 (2008).

⁴M. Hayashi, L. Thomas, C. Rettner, R. Moriya, and S. S. P. Parkin, *Nat. Phys.* **3**, 21 (2007).

⁵M. Hayashi, L. Thomas, C. Rettner, R. Moriya, and S. S. P. Parkin, *Appl. Phys. Lett.* **92**, 112510 (2008).

⁶M. Diegel, R. Mattheis, and E. Halder, *Sens. Lett.* **5**, 118 (2007).

⁷S. Glathe, I. Berkov, T. Mikolajick, and R. Mattheis (unpublished).

⁸D. V. Berkov and N. L. Gorn, MICROMAGUS, package for micromagnetic simulations (www.micromagus.de).

⁹J.-Y. Lee, K.-S. Lee, S. Choi, K. Y. Guslienko, and S.-K. Kim, *Phys. Rev. B* **76**, 184408 (2007).

¹⁰A. Thiaville and Y. Nakatani, in *Spin Dynamics in Confined Magnetic Structures III*, edited by B. Hillerbrands and A. Thiaville (Springer, New York, 2006), p. 161.

¹¹M. T. Bryan, T. Schreffl, D. Atkinson, and D. A. Allwood, *J. Appl. Phys.* **103**, 073906 (2008).